

Numerical Modeling of Optical Parametric Chirped Pulse Amplification to Design a Petawatt Laser Front End

by Josh Keegan

LLE Advisor: Mark Guardalben

Abstract

A numerical model of optical parametric chirped pulse amplification (OPCPA) was developed and used to investigate two designs for the front end of a proposed petawatt laser, which is a very high intensity laser. A petawatt laser is required for fast ignition, a new technique that has the potential to greatly benefit the study of Inertial Confinement Fusion (ICF) and is being investigated at various laboratories around the world. The first design, which is for a proof-of-principle experiment, was one which attempts to preserve the spectral characteristics of the input pulse in order to obtain a short temporal pulse width upon recompression. The second design, which is for the actual petawatt laser system, was one which modifies the spectral characteristics of the input pulse in a way that is desirable for injection into the glass amplifier chain. In both cases the number of crystal stages required and the approximate crystal lengths were determined using the model. The proof-of-principle design requires four crystals of BBO while the actual front end system design requires three longer BBO crystals.

1. Introduction

Inertial Confinement Fusion (ICF) is of interest as a possible energy source, and studies

of ICF are in progress in several laboratories around the world, including the University of Rochester Laboratory for Laser Energetics (LLE) and the Lawrence Livermore National Laboratory in the U.S., and Rutherford Appleton Laboratory in the U.K. In ICF, a target filled with deuterium and tritium is illuminated with a high-intensity laser pulse, causing a fusion reaction of the deuterium and tritium atoms that produces helium atoms and high-energy neutrons as by-products. This process is initiated by ablation of the target shell, which according to Newton's Third Law produces an opposite and equal reactive force that implodes the fuel at the center of the target, compressing it to higher density. Uniformity of the incident laser beams and the target surface are necessary to produce the central ignition hot spot. ⁽¹⁾

Fast ignition is a new technique that has the potential to increase overall efficiency while decreasing the requirements for uniformity of illumination and the target surface ⁽¹⁾. Studies of fast ignition are now in progress in various countries around the world, including Japan, Germany, England, and France ⁽²⁾. In the fast-ignition concept, a laser having a long pulse width ($\sim 10^{-8}$ s) compresses the target while a petawatt (10^{15} W) laser having a short pulse width ($\sim 10^{-12}$ s) is used to heat the target at the point of maximum target compression. The amplification stages of a petawatt laser system are shown in Fig. 1: a seed pulse having low energy is produced by a laser oscillator and injected into a front end amplification stage. A glass amplifier chain further amplifies the laser pulse until sufficient energy is achieved, at which point the pulse is delivered to the target.

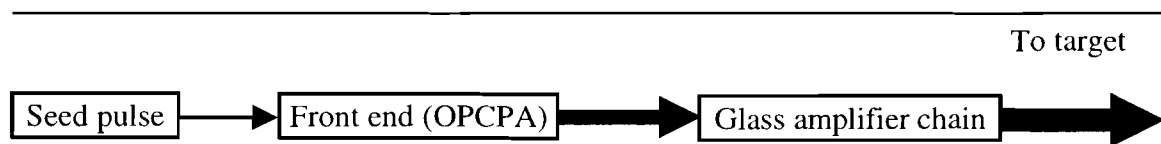


Fig. 1. Petawatt laser amplification stages. A low-energy pulse produced by an oscillator is amplified by the front end, which in this case will use OPCPA. The front end output pulse is injected into a Nd:glass amplifier chain for further amplification and eventual delivery to the target.

Optical parametric chirped pulse amplification (OPCPA) is currently under consideration as a possible front end amplification technique. In OPCPA a short pulse (~100 fs) is temporally stretched using diffraction grating pairs (to ~5 ns), lowering the power of the input pulse while preserving the pulse's total energy*, thereby allowing higher pulse energy after amplification without damage to the gain medium. The stretched pulse is amplified by propagation through several stages of nonlinear optical crystals and a glass amplifier chain, after which it is recompressed with another diffraction grating pair and delivered to the target. OPCPA is proposed as the front end amplification technique because preservation of bandwidth is essential to obtain good recompression, and OPCPA is a broadband amplification technique (meaning that there is little loss of bandwidth). The gain bandwidth of Nd:glass amplifiers is too small to be used as a front end amplifier.

A model of OPCPA which solves the coupled wave equations by numerical integration was created and used to investigate two designs for the front end of a petawatt laser system which is being proposed for integration into the OMEGA laser at the University of Rochester Laboratory for Laser Energetics. In each case various design parameters were determined, including the number and approximate length of crystal stages required for various output pulse energies and spectra. In the first design for a proof-of-principle experiment to demonstrate the OPCPA technique, four BBO crystals were used for a total crystal length of 32.7 mm, while in the front end design for the actual system three BBO crystals with a total length of 39 mm were used. In both cases a 1 nJ pulse was amplified to 300 mJ. Both designs were optimized for efficiency. The proof-of-principle design uses 2.61 J of pump energy while the actual system design uses 1.90 J of pump energy.

* There is a slight energy loss on the grating; some gratings have efficiencies ~ 96%

2. Theoretical Description of OPCPA

The amplification and subsequent recompression of chirped optical pulses was first demonstrated by Strickland and Mourou at LLE in 1985.⁽³⁾ The current implementation of chirped pulse amplification (CPA) uses paired diffraction gratings to temporally stretch the pulse and an additional set of gratings in a different configuration to recompress the pulse after amplification (see Fig. 2).

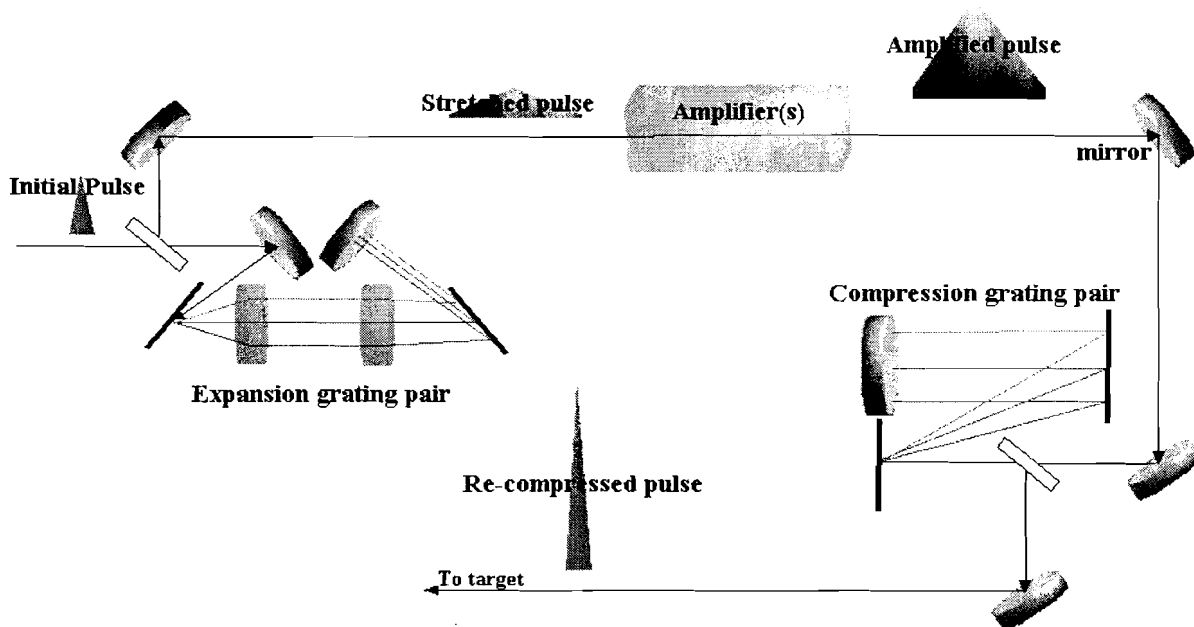


Fig. 2. Overview of CPA. A short, low-energy pulse is temporally stretched using paired diffraction gratings, amplified, and then recompressed, again using diffraction gratings. This technique leads to a very high-power recompressed pulse without damage to the gain medium or other optics.

Shorter temporal laser pulses must necessarily contain a broader spectrum due to the Fourier relationship between time and frequency. The expansion grating pair is configured such that the shorter wavelengths of the pulse spectrum travel a longer distance, causing the pulse to be stretched in time and lowering the pulse peak intensity, thus reducing the potential for damage to the gain medium. This means that the longer wavelengths are at the front of the pulse while the shorter wavelengths are at the end. The process used in the compression grating pair is

similar to that used in the expansion grating pair although a different configuration causes the longer wavelengths of the pulse spectrum to travel longer distances, essentially canceling the effect of the expansion grating pair. However, amplification of the pulse prior to recompression results in a recompressed pulse of very high peak intensity.

The amplification process in OPCPA is difference–frequency generation in a nonlinear optical crystal (see Fig. 3).

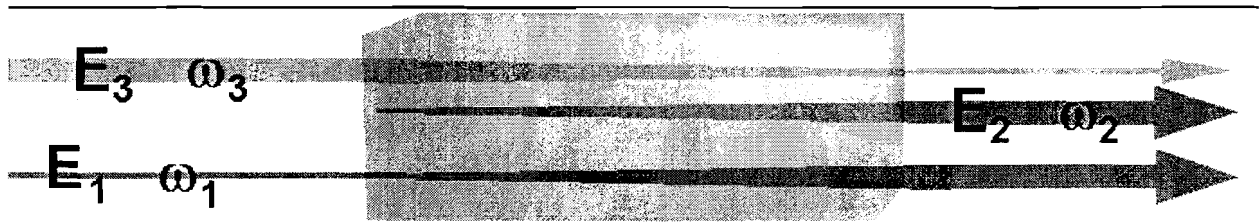


Fig. 3. Difference–frequency generation in a nonlinear optical crystal. Throughout the process, pump beam (E_3) weakens, signal beam (E_1) gains energy, and idler beam (E_2) is generated.

In difference–frequency generation the signal beam gains energy from the pump beam during propagation through the crystal through a nonlinear optical process whereby one photon of the pump beam is converted into one photon of the signal beam and one photon of the idler beam. Following the law of energy conservation, the idler beam that is generated by the process has a frequency given by $\omega_2 = \omega_3 - \omega_1$ where ω_2 is the frequency of the idler, ω_3 is the frequency of the pump, and ω_1 is the frequency of the signal.

A type I process was modeled, meaning that the pump was an e–wave and the signal and idler were o–waves. An e–wave has an electric field component along the crystal’s optic axis while an o–wave does not. The coupled wave equations that describe the transfer of energy in the crystal are given as ⁽⁴⁾:

$$\frac{dE_1'}{dz} = -\frac{1}{2} \gamma_1 E_1' - iK E_3' E_2'^* \cdot e^{-i\Delta k z} \quad (1)$$

$$\frac{dE_2'}{dz} = -\frac{1}{2} \gamma_2 E_2' - i(\omega_2/\omega_1) K E_3' E_1'^* \cdot e^{-i\Delta k z} \quad (2)$$

$$\frac{dE_3'}{dz} = -\frac{1}{2} \gamma_3 E_3' - i(\omega_3/\omega_1) K E_1' E_2' \cdot e^{i\Delta k z} \quad (3)$$

$$\text{where } \Delta k = \frac{\omega_3 n_3 - \omega_2 n_2 - \omega_1 n_1}{c} \quad (4)$$

and K is the nonlinear coupling coefficient. Here $E_j' = \sqrt{n_j} E_j$, the n_j are refractive indices, the γ_j are absorption coefficients for $j=1-3$, and the electric fields are given by the real parts of $E_j e^{(i\omega_j t - ik_j z)}$, with the E_j slowly varying functions of z . c is the speed of light in meters per second. For the wavelengths used (1054 nm signal and 532 nm pump), $K=8.38793 \times 10^{-7} \text{ V}^{-1}$ for KDP⁽⁴⁾ and $K=6.11270 \times 10^{-6} \text{ V}^{-1}$ for BBO⁽⁵⁾.

The refractive indices can be calculated with the use of appropriate Sellmeier equations, which describe the principle refractive indices for e- and o-waves as functions of wavelength (n_e and n_o , respectively). The refractive indices for the signal and idler beams (n_1 and n_2) are simply the principle refractive indices for o-waves of the appropriate wavelengths. The refractive index of the pump is given as $n_3 = n_e n_o \cdot (n_e^2 \cos^2 \vartheta + n_o^2 \sin^2 \vartheta)^{-1/2}$ where ϑ is the angle between the wave vector of the pump and the optic axis of the crystal. The phase-matching angle ϑ_m is by definition the angle at which the phase mismatch Δk , given by Eq. 4, is zero. For BBO the phase-matching angle is calculated as $\vartheta_m = 22.7856^\circ$, while for KDP $\vartheta_m = 41.2097^\circ$. Energy transfer is most efficient when $\Delta k = 0$, so the crystals must be cut at the phase-matching angle.

The coupled wave equations (Eqs. 1-4) were solved numerically using the halfstep-

wholestep process. The program was tested by comparison with the analytical solutions of the coupled wave equations, which assume a constant pump and no absorption:

$$E_1'(z) = E_1'(0) \cosh(gz) \quad (5)$$

$$E_2'(z) = -i \sqrt{\frac{\omega_2}{\omega_1}} \frac{E_3'}{|E_3'|} E_1'(0)^* \sinh(gz) \quad (6)$$

$$g = \sqrt{\frac{\omega_2}{\omega_1}} K |E_3'| \quad (7)$$

3. Numerical Model of OPCPA

The numerical model was used to investigate parametric amplification in crystals of KDP and BBO for use in a petawatt laser system. However, the model is very flexible and can easily accommodate any crystal type given appropriate Sellmeier equations and nonlinear coupling constants, which can be found in Ref. 5. Any wavelengths of incident light for which the Sellmeier equations remain valid can be modeled, but typically a 532 nm pump and a signal with a central wavelength of 1054 nm were used. Currently, pumps with flat-top and Gaussian temporal shapes have been modeled; however, the pump's temporal shape can easily be modified given the equation of a theoretical shape or data on an experimentally measured shape. Any number of crystal stages can be modeled by adding length and crystal type specifications for additional stages (it is assumed that the aperture is large enough to accommodate the beam spot size). The beam spot size is also taken into account when determining the intensity (and therefore electric field values) of the pump and signal, although the beams are assumed to have a flat-top spatial profile. The phase-matching angle, ϑ_m , can be calculated for any crystal type and wavelength.

To model the temporal stretching of the pulse, the Fourier transform of the input pulse was taken, and a stretched pulse was created by assigning a temporal delay $\Delta \tau$ to each spectral mode $\Delta \omega$ using ⁽⁶⁾:

$$\Delta \tau = \frac{-1}{\mu} \Delta \omega \quad . \quad (8)$$

Here $\mu = \frac{\omega_0^3 d^2 \{1 - [(2\pi c / \omega_0 d) - \sin \gamma]^2\}}{4\pi^2 c b}$ where ω_0 is the central frequency of the incident

light, d is the distance between adjacent grooves of the gratings (675 nm), γ is the angle between the incident beam and the normal of the grating (48°), and b is the distance between the two gratings (13 m). Values for γ , b , and d were chosen to lead to a stretched pulse width which meets the design requirement of approximately 5 ns. The inclusion of imaging lenses between the expansion gratings produces a virtual image of the first grating, causing the effective distance between the gratings (b) to be negative in the expansion grating pair. This gives

$\mu^{-1} = \pm 1.77 \times 10^{-22} \text{ s}^2$, depending on which grating pair is under consideration.

This allowed each spectral mode of the transformed pulse to be uniquely mapped to one temporal point of the pump beam through the scaling factor $-\mu^{-1}$. The electric field values of the transformed pulse were then multiplied by a normalization factor such that the spectral pulse contained the correct energy. A graph of stretched (chirped) pulse intensity and frequency vs. time can be found in Fig. 4.

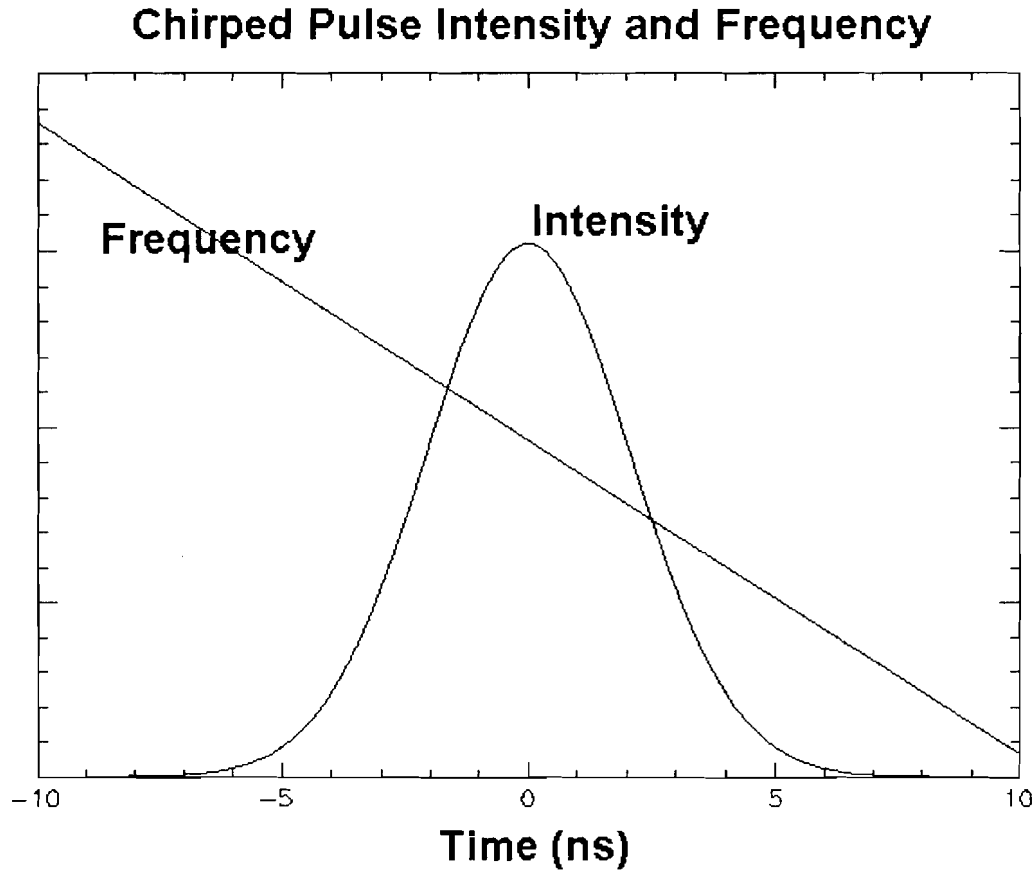


Fig. 4. Graph of intensity and frequency vs. time for a temporally stretched (chirped) pulse. The plot of intensity as a function of time is a perfect Gaussian while the frequency varies linearly with time.

The pulse was then propagated through the crystal stages, using (Eq. 8) to determine which frequencies of the signal should interact with various temporal points of the pump. After propagation through the crystal stages the inverse transform was taken, resulting in a recompressed pulse with a short temporal width.

The results obtained from the numerical model matched the results obtained from the analytical solutions (Eqs. 5–7) of the coupled wave equations in the small–signal regime, after which the models diverged due to pump depletion (see Fig. 5). Therefore the numerical model is needed to design a system which does not operate in the small–signal regime.

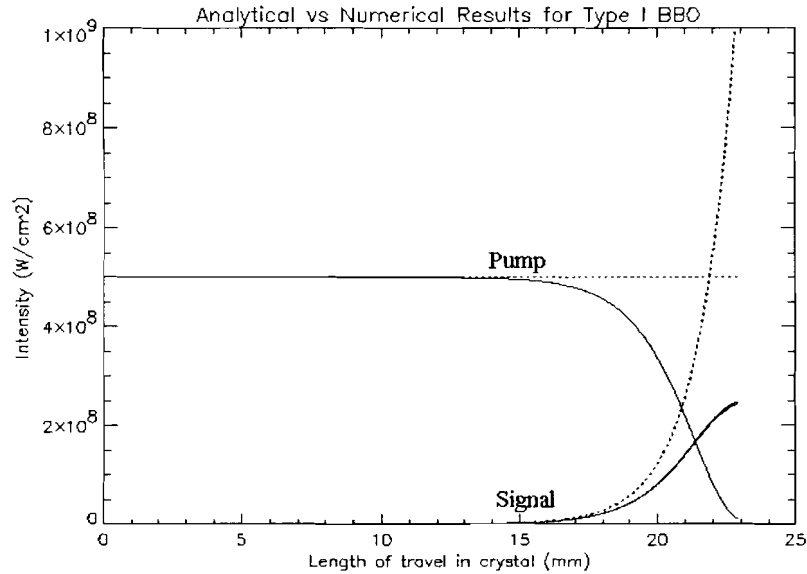


Fig. 5. Plot of intensity vs. length of travel in BBO crystal for analytical results (dotted line) and numerical results (solid line) shows that the models agree in the small-signal regime, after which they diverge due to pump depletion.

4. Design for proof-of-principle experiment

The numerical model was used to investigate designs for a petawatt laser front end leading to a high-quality (i.e., short) recompressed front end output pulse. This design was for proof-of-principle, and an experiment is planned to compress the OPCPA output without injecting it into the glass amplifier chain to determine if the system behaves as predicted and to see if a short recompressed pulse can be obtained.

The goals of the design were to amplify a 100 fs pulse with 1 nJ of energy to at least 250 mJ using 3 J or less of pump energy per crystal stage, with a relatively short recompressed pulse and a pulse contrast of about 10^5 or 10^6 . High pulse contrast is desirable for target illumination – lower pulse contrast means a higher prepulse level, which may perturb the target prior to arrival of the main pulse and detrimentally affect the fusion process. To obtain a short recompressed

pulse with a high pulse contrast level, a spectral shape which is very close to a Gaussian is required, and since the input pulse is a Gaussian in time (and therefore frequency) the required amplification must be performed with as little modification to the spectrum as possible.

A single-crystal example can be used to illustrate the basic design considerations. A flat-top pump, which can be approximated by a Gaussian pump of a large width (a 32 ns pump was used in the first two stages), is required to preserve the spectrum in the small-signal regime*. A flat-top pump preserves the signal spectrum in the small-signal regime because the analytical solutions (Eqs. 5–7) remain valid, and if the intensity of the pump does not vary with time then there will be an equal multiplication of all temporal points of the signal electric field, leading to a flat signal gain profile. However, due to the fact that energy is transferred more quickly from the pump to the signal at the center of the pulse, pump depletion affects the pump to a greater extent in the center than in the temporal wings. This causes distortions to the spectrum of the signal to be present if significant depletion occurs, which leads to lower pulse contrast after recompression (see Fig 6). The goal of the design is to extract the greatest amount of pump energy possible without compromising the recompressed pulse contrast – for the pump and signal energies used to generate Fig. 6, a 22 mm crystal results in high gain with moderate distortions to pulse shape, while a 25 mm crystal results in even higher gain, but at the cost of large distortions to the spectrum and therefore the recompressed pulse shape.

The trade-off between recompressed pulse contrast and efficiency was the primary consideration in the design of the proof-of-principle system. Using the model, a four-stage system was designed (relevant design parameters may be found in Table 1).

* Slight distortions of the spectrum occur due to phase mismatch even with a flat-top pump

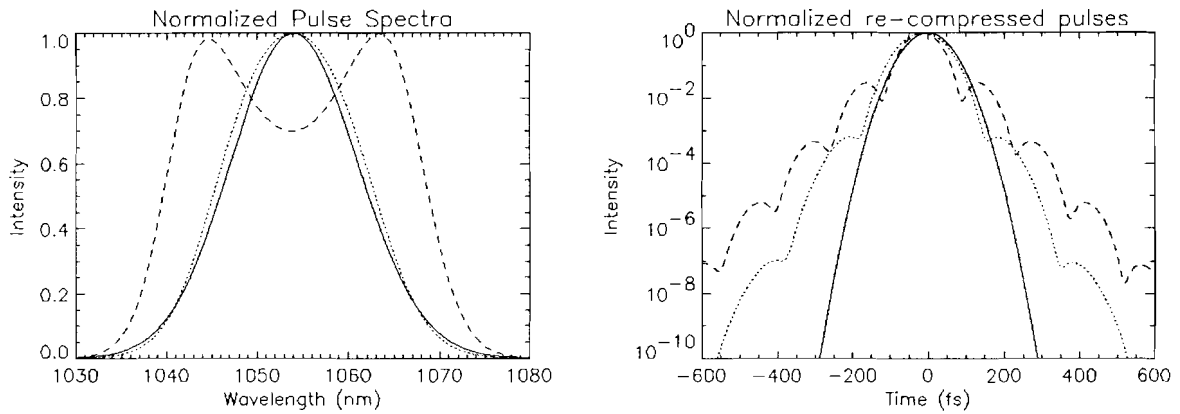


Fig. 6. Normalized pulse spectra (left) and recompressed pulse intensity (right) show how spectral shape affects recompression. Shown are an initial pulse (solid line), a pulse after 22mm of BBO crystal (dotted line), and a pulse after 25mm of BBO crystal (dashed line). Pump depletion modifies the spectral characteristics of the pulse cumulatively, resulting in an increasingly poor recompressed signal with increasing pump depletion.

Table 1. Values used in the different crystal stages for the proof-of-principle design

	Stage 1	Stage 2	Stage 3	Stage 4
Crystal (BBO)	4x4x14.5mm	5x5x9.5mm	7x7x4.5mm	10x10x4.2mm
Sig/Pump Spot Size	0.4mm/1.2mm	2.8mm/3.3mm	5.6mm/5.9mm	8.0mm/8.2mm
Pump	115mJ, 32ns	780mJ, 32ns	888mJ, 8ns	829mJ, 4.5ns
Pump max Intensity	237 MW/cm ²	213 MW/cm ²	314 MW/cm ²	264 MW/cm ²
Input / Output	1nJ / 22.4μJ	22.4μJ / 6.50mJ	6.50mJ / 70.7mJ	70.7mJ, 300mJ
Gain	22400	290.2	10.9	4.4
Efficiency	0.02%	0.83%	7.22%	27.63%

This system uses a total of 2.61 J of pump energy to amplify a 1 nJ, 100 fs pulse to 300 mJ. The design goal of 250 mJ was intentionally exceeded to compensate for secondary gain-reducing effects which are not yet taken into account. All four stages were modeled using BBO as a gain medium due to its large nonlinear coupling constant. The maximum pump intensity in any crystal stage was 314 MW/cm², thus the damage threshold of BBO for 532 nm light (500–1000 MW/cm² ⁽⁷⁾) was not exceeded. The final recompressed pulse had a pulse width of 203 fs

and a pulse contrast of $\sim 10^5$. The pulse spectra throughout the crystal stages and the final recompressed pulse are shown in Fig. 7.

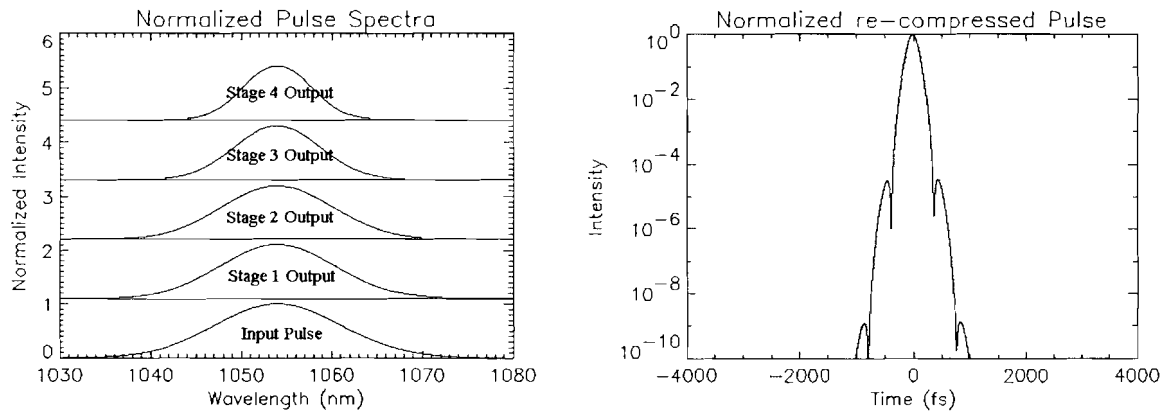


Fig. 7. Normalized pulse spectra (left) and recompressed pulse intensity (right) for proof-of-principle design. Recompressed pulse width is 203 fs, energy is 300 mJ.

It was determined that four stages were needed for this design, as it was possible to meet the output energy requirement using three stages, but only at the cost of recompressed pulse contrast. After approximate crystal lengths and pump energies were determined, each stage was optimized individually, beginning with the first stage. In optimizing the system, stages were added one at a time so that their effect on the recompressed pulse could be easily seen. In the first two stages the spectral pulse shape was preserved to the greatest extent possible by operating far from pump depletion, which led to an almost perfect recompressed pulse at the output of the first two stages. A very wide pump (32 ns) was used for both of these stages to preserve signal bandwidth to the greatest extent possible, which, combined with operating far from depletion, led to very low efficiency. In the final stages much shorter pump pulses were used both to increase efficiency (since less energy is wasted in the wings where there is almost no signal to amplify) and to help maintain the Gaussian shape of the spectrum. Much shorter crystals were used in these stages because the higher initial signal intensities led to a much more rapid transfer of energy. Depletion in these stages led to distortions of the pulse spectrum and therefore higher

levels of prepulse. All pump spot sizes are larger than the signal spot sizes to compensate for walk-off, which will be discussed later. The pump and signal beam spot sizes are increased between crystal stages to lower intensity and therefore potential for damage to the gain medium.

5. Design for petawatt system

For the petawatt system, a design was needed to produce a flat-top spectrum output pulse for injection into the Nd:glass amplifier chain. This is desirable because gain narrowing in the amplifier chain can reduce the pulse pedestal, increasing pulse contrast⁽⁸⁾. The glass amplifiers were modeled with a transfer function which assumes a small-signal gain of about 2200*. The transfer function used was a Gaussian centered at 1052.57 nm with a FWHM of 5.2 nm. Using this design, a front end output of 300 mJ was obtained in three crystal stages using a total pump energy of 1.90 J. See Table 2 for relevant design parameters.

Table 2. Values used in different stages for the petawatt system design

	Stage 1	Stage 2	Stage 3
Crystal	4x4x16 mm BBO	5x5x15 mm BBO	10x10x8 mm BBO
Sig/Pump Spot Size	0.4 mm / 1.3 mm	2.8 mm / 3.6 mm	8 mm / 8.4 mm
Pump	49.0 mJ, 16 ns	333 mJ, 16 ns	1.52 J, 16 ns
Pump Max Intensity	203 MW/cm ²	152 MW/cm ²	128 MW/cm ²
Input / Output	1 nJ / 23.1 μJ	23.1 μJ / 30.6 mJ	30.6 mJ, 300 mJ
Gain	23100	1324.7	9.8
Efficiency	0.05%	9.19%	17.77%

The final recompressed pulse width after the glass amplifier chain was 798 fs. This is much greater than the 203 fs obtained from the proof-of-principle design, but still well within the design goal of 1 ps. The recompressed pulse is much longer due to gain narrowing in the glass amplifier chain. Flat-spectrum pulses are more easily obtained at the output of OPA than

* Pulse shape was modeled using the transfer function, but energy was normalized, producing a gain of 1

are Gaussian-spectrum pulses because pump depletion lowers gain in the center of the pulse before lowering gain in the wings, essentially flattening out the spectrum. The pulse spectra throughout the crystal stages and the final recompressed pulse are shown in Fig. 8. The recompressed pulse contrast was higher than 10^{10} at ± 2 ps.

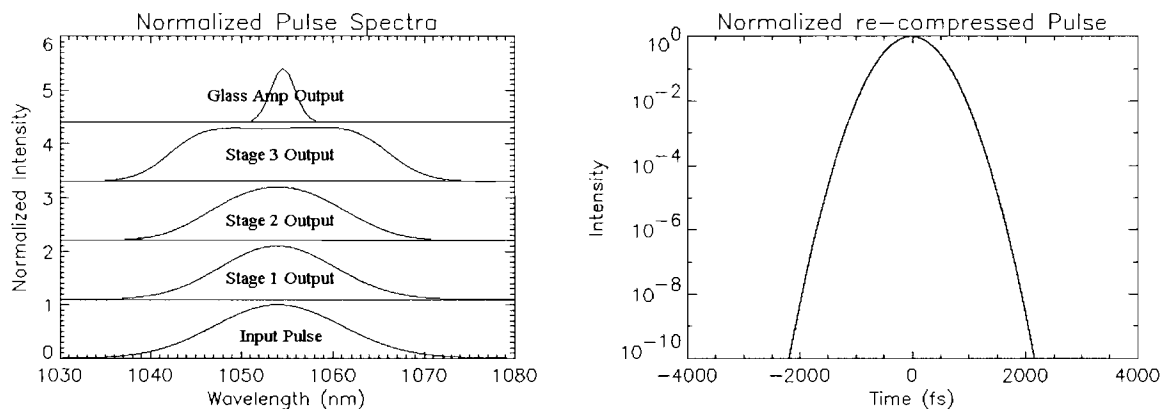


Fig. 8. Normalized pulse spectra (left) and recompressed pulse intensity (right) for actual system design. Recompressed pulse width is 798 fs, well within the design goal of 1 ps. Final output energy is 300 mJ.

Table 3 contains a comparison of the two designs. In the actual system design three crystal stages were required instead of four because the pumps can be run farther into depletion (the effects associated with pump depletion in the proof-of-principle design are now actually desirable for this design). This requires longer crystals but less pump energy, allowing for higher overall efficiency (defined as the total increase in signal energy over the total pump energy used). Preservation of bandwidth was a secondary concern in the actual system design because injection into the Nd:glass amplifiers will reduce bandwidth anyway. As in the proof-of-principle design, stages were added and optimized individually, and the signal and pump beam spot sizes are expanded between crystal stages.

Table 3. Comparison of proof-of-principle and actual system designs

	Proof-of-principal design	Actual system design
Number of rystals	4	3
Total crystal length	32.7 mm	39 mm
Pulse width (Input / Output)	100 fs / 202 fs	100 fs / 798fs
Pump width	32–4.5 ns	16 ns
Total pump energy used	2.61 J	1.90 J
Signal energy (Input / Output)	1 nJ / 300 mJ	1 nJ / 300 mJ*
Overall efficiency	11.50%	15.79%

* Energy of output pulse before glass amplifier chain

The capability to run the actual system design farther into depletion led to increased efficiency due to the fact that much less pump energy had to be used since more of it was extracted. The output pulse width is much larger for the actual system design due to loss of bandwidth in the Nd:glass amplifier chain, but the design goal of less than a picosecond was still met.

6. Future work

In the future the model will be improved to include several other capabilities. The ability to model the spatial shapes of the beams will be added, as well as the walk-off (lateral displacement) of the pump. Walk-off in an anisotropic crystal occurs because the Poynting vector of the e-wave (direction of energy flow) is not the same as the k-vector (the vector normal to the wavefront). This affects only the pump and not the signal and idler because only the pump is an e-wave (the signal and idler beams are o-waves). The walk-off angle in BBO is ~3 degrees, which has been taken into account in only a limited way in that the pump spot sizes are larger than the beam spot sizes to maintain overlap throughout the crystal. However, this effect is more prevalent in the first stage because the spot size is smaller and walk-off is greater due to the longer path through the crystal.

The capability to model a non-collinear angle between the pump and signal beams will be included. Reasons for using a non-collinear angle include being able to separate the signal and idler beams after propagation through the crystal, compensating for walk-off, and larger gain bandwidth ⁽⁹⁾.

The B-Integral, which refers to the accumulated nonlinear phase (self-phase modulation) and is defined as

$$B = \frac{2\pi}{\lambda} \int n_2 I dl$$

will also be taken into account. Here n_2 is the nonlinear refractive index, I is the intensity of the beam, and dl is the incremental crystal length. The phase of the incoming light is not changed equally across the whole beam, but changes in part as a function of intensity. This effect can occur across both time and space because intensity varies across both time and space.

Therefore the temporal effects of the B-Integral could be included in the current model without considering spatial dependence. Nonuniform phase accumulation across the beam can cause a self-focusing effect which produces areas of differing intensity, possibly leading to damaged optics. The effect of accumulated nonlinear phase is expected to be small, however, due to the short path through the gain medium. In work done by Jovanovic ⁽¹⁰⁾ using similar crystal lengths, intensities, and signal energy as the two designs reported here, nonlinear phase accumulation was 0.04 radians and had a negligible effect.

The effect of group velocity difference between the three beams (caused by their different wavelengths and polarizations) may also eventually be considered. However, its effect is expected to be small.

The numerical model will also be used to investigate the stability of the system (to determine the range of of output pulse energy fluctuations for a given range of pump energy

fluctuations) and the sensitivity of the system to angular detuning (to establish the tuning tolerance).

7. Conclusions

A numerical model of OPCPA was developed and used to design two petawatt laser front ends, one which leads to a short recompressed pulse for a proof-of-principle experiment and one which leads to spectral characteristics desirable for injection into the main Nd:glass amplifier chain of the petawatt laser being designed at the University of Rochester LLE. Both designs amplified the pulse to 300 mJ, exceeding the design goal of 250 mJ. The width of the recompressed pulse from the glass amplifier chain (798 fs) was well within the design goal (1 ps). Optimized versions of these designs including secondary effects such as walk-off and non-collinear propagation will be used for the design of the petawatt laser system which will be incorporated into the OMEGA laser system as an implementation of the fast-ignitor concept. A fast ignitor has the potential to increase the efficiency of ICF, bringing nuclear fusion a step closer to use as an effective energy source.

Acknowledgments

I would like to thank Dr. Stephen Craxton for giving me the opportunity to participate in the High School Summer Research program at the University of Rochester Laboratory for Laser Energetics, and for all the work he spent making the program so successful. I would also like to thank my advisor, Mark Guardalben, who spent many hours teaching me the concepts behind OPCPA; his assistance has been invaluable in completing this project and without it this project would not have been possible.

References

- (1) – Michael H. Key, "Fast Track to Fusion Energy," *Nature* **412**, 775–776 (2001).
- (2) – L. Waxer and J. Kelly, "Conceptual Fast–Ignitor System Design", presentation given at LLE April 4, 2001.
- (3) – D. Strickland and G. Mourou, *Opt. Comm.*, 56 (1985) 219.
- (4) – R. S. Craxton, "High Efficiency Frequency Tripling Schemes for Higher–Power Nd:Glass Lasers," *IEEE Journal of Quantum Electronics* **QE–17 No. 9**, 1771–1782 (1981).
- (5) – V. G. Dmitriev, G. G. Gurzadyan, and D. N. Nikogosyan. Handbook of Nonlinear Optical Crystals. Berlin Heidelberg, Germany: Springer–Verlag, 1991, 1997, 1999.
- (6) – Edmond B. Treacy, "Optical Pulse Compression with Diffraction Gratings," *IEEE Journal of Quantum Electronics* **QE–5 No. 9**, 454–458 (1969).
- (7) – Igor Jovanovic, Brian J. Comaskey, Chris A. Ebbers, Randal A. Bonner, Deanna M. Pennington, Edward C. Morse, "Optical Parametric Chirped Pulse Amplifier as an Alternative to Ti:sapphire Regenerative Amplifiers," to be published.
- (8) – M.D. Perry, F.G. Patterson, and J Weston, "Spectral shaping in chirped–pulse amplification," *Opt. Lett.* 15, 381 (1990).
- (9) – Pavel Matousek, Bedrich Rus, and Ian N. Ross, "Design of a Multi–Petawatt Optical Parametric Chirped Pulse Amplifier for the Iodine Laser ASTERIX IV," *IEEE Journal of Quantum Electronics* Vol 32 No 2, 158–162 (2000).
- (10) –I Jovanovic, B J Comaskey, C A Ebbers, R A Bonner, D M Pennington, "Replacing Ti:sapphire regenerative amplifiers with an optical parametric chirped pulse amplifier," CPD8–1, CLEO 2001 Post–deadline conference, May 6–11, 2001, Baltimore Convention Center.